

Empirical model for estimating groundwater flow into tunnel in discontinuous rock masses

Hadi Farhadian^{1,2} · Homayoon Katibeh¹ · Peter Huggenberger²

Received: 21 July 2015 / Accepted: 28 November 2015 / Published online: 10 March 2016
© Springer-Verlag Berlin Heidelberg 2016

Abstract The high volume of water inflow into tunnel plays a significant role in the design of drainage systems and exerts bio-environmental effects. In engineering practice, analytical and empirical methods that are commonly used to estimate water inflow in sedimentary rock masses, lack sufficient accuracy. The geostructural anisotropy in a fractured rock has a great impact on water inflow. In discontinuous media, anisotropy and heterogeneity of the fractured rock masses are highlighted. Hence, these methods are not efficient to calculate water inflow to tunnel in such media, due to the assumed isotropic hydraulic coefficient. In this regard, an empirical formula is developed in this study for hydraulic conductivity in the fractured rock masses for analytical methods, alternately used to predict water inflow. To achieve this, a discrete network flow model was performed. The simulation resulted in a dataset that is helpful in developing hydraulic conductivity empirical formula for well-known Goodman equation. The geostructural parameters, such as the joint orientation, aperture, spacing and joint interconnectivity were included to determine this formula. The acquired empirical equation

was utilized in the evaluation of groundwater inflow to middle-depth Amirkabir tunnel in north of Iran. In comparison to the observed flow, analytical methods resulted in higher overestimation, especially in the sites with high anisotropy. However, empirical model led to a better estimation of water inflow to tunnel.

Keywords Groundwater flow · Fractured rock · Analytical equation · Numerical modeling · Amirkabir tunnel

List of symbols

\varnothing_{\min}	Angle between direction minimum components of the hydraulic conductivity and the horizontal plane (°)
K_w	Bulk modulus of the fluid (Pa)
i	Cluster number of fracture
R	Correlation coefficient
a_i	Corner of normal direction of fracture and coordinate axis
R^2	Coefficient of determination
P_c	Critical probability
h	Depth of the tunnel centre from the water table (m)
μ	Dynamic viscosity of the fluid (Pa s)
g	Earth Gravity (m/s^2)
K_{sim}	Empirical hydraulic conductivity (m/s)
Q_{em}	Empirical tunnel inflow (m^3/s)
K_{eq}	Equivalent hydraulic conductivity (m/s)
a	Fracture aperture (m)
K	Hydraulic conductivity (m/s)
H	Hydraulic head into the tunnel (m)
P	Interconnectivity probability
ν	Kinematics viscosity of water (m^2/s)
l	Length assigned to the contact between the domains (m)

✉ Homayoon Katibeh
Katibeh@aut.ac.ir

Hadi Farhadian
Farhadian@aut.ac.ir; Hadi.farhadian@unibas.ch

Peter Huggenberger
Peter.huggenberger@unibas.ch

¹ Department of Mining and Metallurgical Engineering, Amirkabir University of Technology (Tehran Polytechnic), 424 Hafez Ave., P.O. Box 44113-15875, Tehran, Iran

² Applied and Environmental Geology, Department of Environmental Sciences, University of Basel, Bernoullistrasse 32, 4056, Basel, Switzerland

a_{\max}	Joint aperture at maximum value (m)
a_{res}	Joint aperture at minimum value (m)
a_0	Joint aperture at zero normal stress (m)
u_n	Joint normal displacement (m)
K_j	Joint permeability factor, whose theoretical value is $1/12\mu$ (1/Pa s)
K_{\max}	Maximum components of the hydraulic conductivity (m/s)
K_{\min}	Minimum components of the hydraulic conductivity (m/s)
θ_{\min}	Minimum joint dip ($^\circ$)
$\Delta p/l$	Pressure gradient (Pa/s)
b	Spacing interval of fractures (m)
n	Total number of the cluster
L	Tunnel length (m)
r	Tunnel radius (m)

Introduction

Water inflow into tunnels is one of the most challenging issues in rock tunneling, which flows through initial discontinuities and/or is created in tunnel walls. This causes some impediments in progress of tunneling, such as decrease in rock mass stability, extra pressure exerted on permanent and temporary stability systems, destructive effects on geo-mechanical condition of rock, and finally physical and economical disasters (Holmoy and Nilsen 2014). According to Palmstrom and Stille (2007), water inflow is the main issue in the underground excavation, and many factors such as the rock mass permeability and environmental conditions play important roles in this scenario.

As it is impossible to identify all the factors that affect water inflow into tunnels, especially during drilling, it is difficult to anticipate the exact amount of seepage into tunnels. Therefore, analytical methods are mostly used to calculate seepage rate into tunnels because of simplifying assumptions. Some important investigations have been carried out to calculate water inflow into tunnels. Specific solutions have also been used effectively to manage different situations. Ribacchi et al. (2002), for example, introduced a solution for lining tunnel, providing that the hydrostatic load is constant along the tunnel border. Considering the Jacob and Lohman (1952) solution, Marechal and Perrochet (2003) modelled transient groundwater discharge into deep tunnels. El-Tani (2003) used a Mobius transformation and Fourier series to present an analytical solution for a semi-infinite isotropic and homogeneous aquifer drained by a circular tunnel. Park et al. (2008) presented a closed-form analytical solution for the steady-state groundwater inflow into a drained circular tunnel with focus on different boundary conditions. Also, El-Tani (2010)

deliberated an analytical equation for a semi-infinite aquifer drained by a circular tunnel in different heterogeneous aquifer settings using a modified Helmholtz equation.

Analytical equations are developed based on the Darcy's Law and mass conservation (Liu et al. 2012). They consist of parameters like rock mass permeability, water table, tunnel radius, etc. These solutions are invalid under the following conditions:

1. Water inflow around the tunnel is vertical,
2. Rock mass bedding around the tunnel is very variable,
3. Rock mass permeability cannot be exactly identified.

Although still the analytical equations are universally valid for homogeneous and isotropic aquifers but Cesano et al. (2003) proposed a heterogeneity index allowing a qualitative evaluation of groundwater flow into tunnel, whereas Perrochet and Dematteis (2007) recommended an extension for heterogeneous aquifers. However, rock masses are typically anisotropic and heterogeneous media, for which the traditional analytical solutions do not accurately predict water inflow (Zhang and Franklin 1993; Fernandez and Moon 2010). Nevertheless, Gattinoni and Scesi (2010) using numerical simulation and defining special geometrical characteristics of the tunnel and model developed an empirical correction to the analytical formula (Goodman equation) for estimating groundwater flow into tunnel in fractured rock.

In spite of analytical methods, which are a total estimation of seepage, with attention to basic equations of seepage flow and site characteristics, with applications of numerical methods such as Finite Element Method *FEM* and Discrete Element Method *DEM*, water inflow into tunnel can be modeled and then seepage into tunnel in various situations in site can be calculated (Coli and Pinzani 2012).

Unlike analytical methods, these methods are difficult in calculation. Also, they require comprehensive data about the site. Moreover, there are less simplifications and assumptions in these methods. Numerical methods are very complex and application of them is time consuming, however, the results are more precise in comparison to Analytical methods. Numerical simulations, therefore, can help to analyse more complicated situations (Dunning et al. 2004; Gattinoni et al. 2008; Molinero et al. 2002; Hwang and Lu 2007; Zangerl et al. 2008; Gattinoni and Scesi 2010; Butscher 2012; Garzonio et al. 2014).

In this study, numerical model results were used in order to define an empirical relation for calculation of equivalent hydraulic conductivity for the most commonly used analytical formulas using the rock mass geostructural properties. To do this, a discrete fractures network approach was used to simulate the groundwater flow into the tunnel (Cacas et al. 1990; Therrien and Sudicky 1996; Blesent et al. 2009).

In order to facilitate mechanical hydraulic study, the universal distinct element code *UDEC* (Itasca 2011) was used. The distinct element code has the capability to perform the analysis of fluid flow through the fractures of a system of impermeable blocks. A fully coupled hydraulic mechanical analysis could be performed in which fracture conductivity is dependent on mechanical deformation and, conversely, fracture water pressure affect mechanical behavior (Alejano 2014). The simulation results allowed the analysis of the tunnel inflow for different geostructural characteristics (joint sets orientation, spacing, aperture, length and gap) and hydrogeological conditions (tunnel depth in comparison to the water table).

Afterwards, for the same configurations used in the numerical model, tunnel groundwater inflow rates were calculated using the analytical formula of Goodman et al. (1965), valid for an infinite, homogeneous and isotropic aquifer. Model results and analytical formula are compared; not taking into account the anisotropy and heterogeneity of the media, the latter greatly overestimates tunnel inflow. Therefore modified hydraulic conductivity formula should be applied to analytic solutions while considering the geological structural setting.

Materials and methods

General

2-D and 3-D simulation of the flow of each single discontinuity is possible by means of discrete models (Long and Witherspoon 1985; Robinson 1982; Hung and Evans 1985; Rasmussen 1988; Andersson and Dverstorp 1987; Dverstorp and Andersson 1989) using the Navier–Stokes equation (Bear 1993), Kirchoff’s laws for electric circuits (Kraemer and Haitjema 1989) or the model with hydraulically connected circular disks (Cacas et al. 1990). Simulation of the flow in the presence of a series of interconnected bond in two-dimensional model is the simplest form in which the hydraulic head of each site is computed as a weight average of the adjacent sites hydraulic head, each one multiplied by a transmissivity coefficient N_{ij} which is related to the flow between the site i and the site j (Fig. 1):

$$H_0 = (N_{10}H_1 + N_{20}H_2 + N_{30}H_3 + N_{40}H_4)/(\Delta N) \tag{1}$$

If transmissivity T_1 is equal to T_2

$$N_{12} = T_1 = T_2 \tag{2}$$

Assuming T_1 as infinite

$$N_{12} = 2T_1 \tag{3}$$

N_{12} is the harmonic mean of T_1 and T_2 , if their values are different:

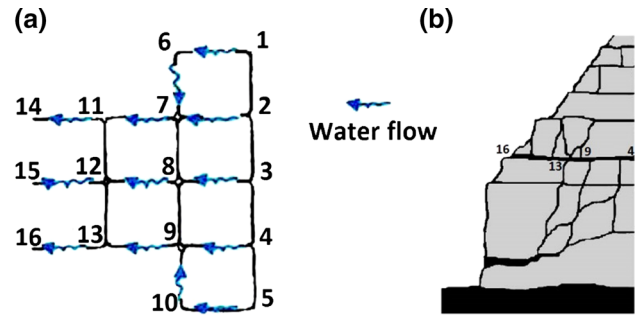


Fig. 1 A 2-D discrete flow model schematization on a plan (a) and in cross section (b) (Croci et al. 2003)

$$N_{12} = (2T_1T_2)/(T_1 + T_2) \tag{4}$$

Numerical modeling of the flow within the single discontinuity is actually performed irrespective of the effects produced by the presence of real shear zones. Numerical distinct element simulation of the groundwater flow requires a comprehensive set of data about the underground and it is frequently used for the investigation of tunnel inflow (Papini et al. 1994; Molinero et al. 2002). *UDEC* is one the best examples of the existing mathematical models simulate waterflow within discontinuities using distinct element method. A hydro-mechanical simulation can also be performed where the joint hydraulic conductivity depends on the mechanical deformation which in turn is influenced by the water pressure inside the discontinuities (Fig. 2) (Itasca 2011).

Detailed data about the discontinuities characteristics must be imported into the numerical distinct element model so that satisfactory results can be obtained. Hence, it is suitable for simulation of local phenomena or detailed scale processes (Samardzioska and Popov 2005).

UDEC is frequently used for simulation of fluid flow through jointed rock media (Herbert 1996; Zhang et al. 1996; Liao and Hencher 1997). Rock blocks surrounded by discontinuities are simulated as rigid or deformable material. In fluid flow simulation, joint conductivity is directly related to the mechanical deformation which is associated with the joint water pressures. Mechanical interaction between blocks is established in where each domain, which is filled with water, is separated by contact points.

In *UDEC*, fluid flow governing equation for steady laminar flow is calculated based on cubic law for a planar fracture as:

$$Q = -\frac{a^3}{12\mu} \cdot \frac{\Delta p}{l} \tag{5}$$

The hydraulic aperture (a) is given, in this analysis, by:

$$a = a_0 + u_n \tag{6}$$

In Fig. 3, the variation of aperture with normal stress on the joint is demonstrated. Opening and closure of joint aperture

Fig. 2 Schematization of the solid–fluid interaction within discontinuities: **a** water discharge; **b** mechanical effects induced by stresses affecting the aperture; and **c** pressure change in the sites (Itasca 2011)

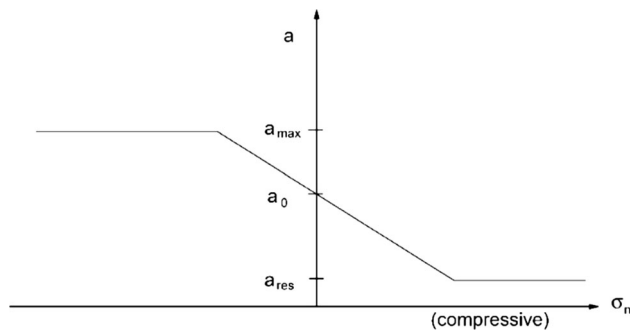
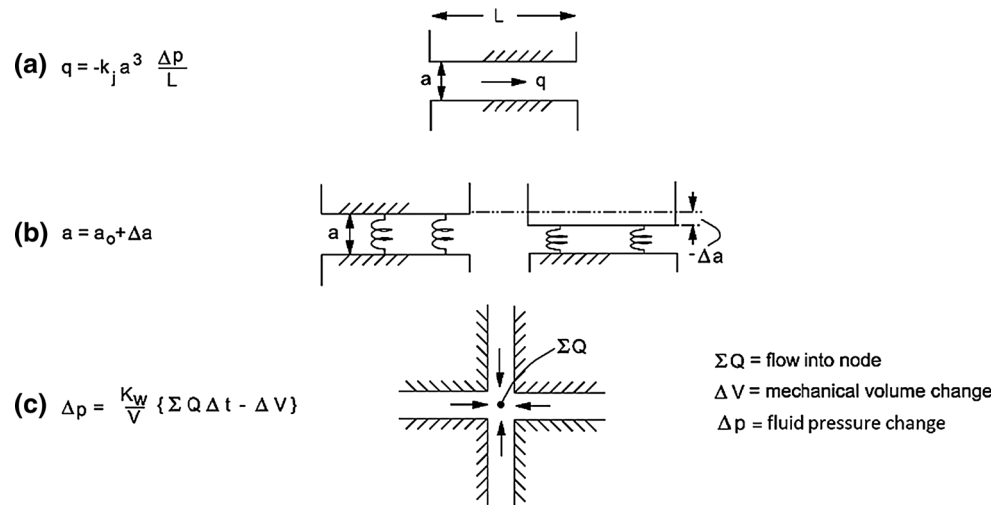


Fig. 3 Hydraulic aperture (a) relation with joint normal stress (n_σ) in UDEC (Itasca 2011)

can be inferred by arithmetic positive and minus signs in Eq. 6, respectively (Itasca 2011).

Numerical modeling procedure

For modeling groundwater flow in a discontinuous media, a rock block was considered (formed from a sedimentary rock or a paragneiss lithotype which is low fractured and karstified) that is crossed by two joint sets with varying orientations, spacing and apertures (Table 1).

The two-dimensional numerical model used in this study includes an assembly of intact rock blocks, different tunnel radiuses, hydraulic head above the tunnel, joint spacing and different joint dip/dip directions.

An intact rock block interacts with adjacent blocks through contacts that are located along two conjugate persistents and equally spaced-joint sets, and the tunnel is intersected by joints as shown in Fig. 4. The initial groundwater table is located immediately below the ground surface. A rectangular domain was chosen ($100 \times 200 \text{ m}^2$) and a tunnel with N–S direction was positioned at its

Table 1 Joint dip direction/dip used for modeling

Joint orientation (dip direction/dip)	K_{eq}	K_{min}/K_{max}	\varnothing_{min}
W/60°–W/45°	0.26	1.74E–02	52.5°
W/60°–W/30°	0.50	7.18E–02	45°
E/5°–W/5°	0.17	7.65E–03	0°
E/10°–W/10°	0.34	3.11E–02	0°
E/0°–W/30°	0.50	7.18E–02	15°
W/60°–W/80°	0.34	3.11E–02	90°
E/20°–W/20°	0.64	1.32E–01	0°
E/15°–W/15°	0.50	7.18E–02	0°
E/0°–W/45°	0.71	1.72E–01	22°
E/25°–W/25°	0.77	2.17E–01	0°
E/10°–E/30°	0.34	3.11E–02	0°
E/0°–W/60°	0.87	3.33E–01	30°
E/30°–W/30°	0.87	3.33E–01	0°
E/10°–E/50°	0.64	1.32E–01	30°
E/40°–W/40°	0.98	7.04E–01	0°
E/0°–W/80°	0.98	7.04E–01	40°
E/0°–E/90°	1.00	1.00E+00	0°
E/15°–W/75°	1.00	1.00E+00	0°
E/45°–W/45°	1.00	1.00E+00	0°
E/25°–W/55°	1.00	1.00E+00	0°
E/40°–W/50°	1.00	1.00E+00	0°
E/70°–w/70°	0.64	1.32E–01	90°
E/85°–W/85°	0.17	7.65E–03	90°
E/80°–W/80°	0.34	3.11E–02	90°
E/50°–W/50°	0.98	7.04E–01	90°
E/75°–W/75°	0.50	7.18E–02	90°
E/65°–W/65°	0.77	2.17E–01	90°
E/60°–W/60°	0.87	3.33E–01	90°

K_{eq} is the equivalent hydraulic conductivity calculated; K_{min}/K_{max} is the anisotropy ratio in the cross sections of the model domain; \varnothing_{min} the angle between K_{min} direction and the horizontal plane

center. For each geo-structural setting considered in the simulations (Table 1), the matrix of permeability tensor $[K]$ based on cubic law (Snow 1969) was calculated:

$$[K] = \begin{bmatrix} 1 - \cos a_x \cos a_x & \cos a_x \cos a_y & \cos a_x \cos a_z \\ \cos a_y \cos a_x & 1 - \cos a_y \cos a_y & \cos a_y \cos a_z \\ \cos a_z \cos a_x & \cos a_z \cos a_y & 1 - \cos a_z \cos a_z \end{bmatrix} \quad (7)$$

a_i ($i = x, y, z$) is the included corner of normal direction of fracture and coordinate axis. If combined actions of all fracture groups are considered, the total rock mass cubic law can be deduced as follows:

$$[K] = \sum_{m=1}^n \frac{ga_m^3}{12b_m\vartheta} \begin{bmatrix} 1 - n_x^m n_x^m & n_x^m n_y^m & n_x^m n_z^m \\ n_y^m n_x^m & 1 - n_y^m n_y^m & n_y^m n_z^m \\ n_z^m n_x^m & n_z^m n_y^m & 1 - n_z^m n_z^m \end{bmatrix} \quad (8)$$

where i is the cluster number of fracture; n is the total number of the cluster; n ($i = x, y, z$) is the normal direction cosine of normal direction of fractures; ϑ is the kinematics viscosity of fissured water 20 °C (10^{-3} Pa \times s); a is the fracture aperture and b is the spacing interval of fractures.

For a more precise and accurate visualization of the rock anisotropy and equivalent hydraulic conductivity calculation, hydraulic conductivity tensor is used (Louis 1974):

$$K_{eq} = (K_1 \cdot K_2 \cdot K_3)^{\frac{1}{3}} \quad (9)$$

where K_1 , K_2 and K_3 are the principal components of the hydraulic conductivity tensor, previously defined.

The universal distinct element code (*UDEC*) was used to evaluate the groundwater inflow into the tunnel. *UDEC* simulates a rock mass as a composition of discrete blocks

separated by joints that are represented by interfaces (Alejano 2014). The parameters used for model implementation are listed in Table 2. In the model, the joint stiffness values were considered independent from the effective normal stress, because the research mainly aimed to study middle-depth tunnels (at an average depth equal to 150 m corresponding to an average normal effective stress in the order of 3 MPa).

For the groundwater flow, the following boundary conditions were applied:

1. A stress boundary condition is created along the top of boundary, with a fixed ratio, k , is defined as the ratio of horizontal to vertical normal boundary stresses. The ratio, k , in this condition is set to be 1.
2. No pore pressure along the top boundary surface as the groundwater table coincides with the top boundary surface. Constant water pressure along the bottom boundary, and linearly increasing the fluid pressure along the left and right vertical surfaces.

The groundwater level above the tunnel can be defined by changing the head assigned to the vertical boundaries. By specifying a constant hydraulic head at these boundaries, drawdown of the groundwater table is balanced by the groundwater recharge in the models as a result of the tunnel inflow. In this study, the groundwater flow into the tunnel was considered to be steady flow.

In the *UDEC* program, the blocks are assumed to be impermeable and the groundwater flows only through the fractures between the impermeable blocks. The groundwater flow in a joint depends on the aperture of the joint, the dip/dip direction joint, the joint spacing that is, in turn, affected by the pore water pressure within the joint (hydro-

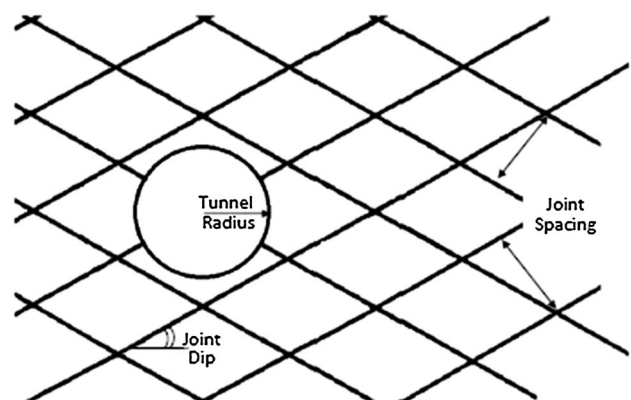
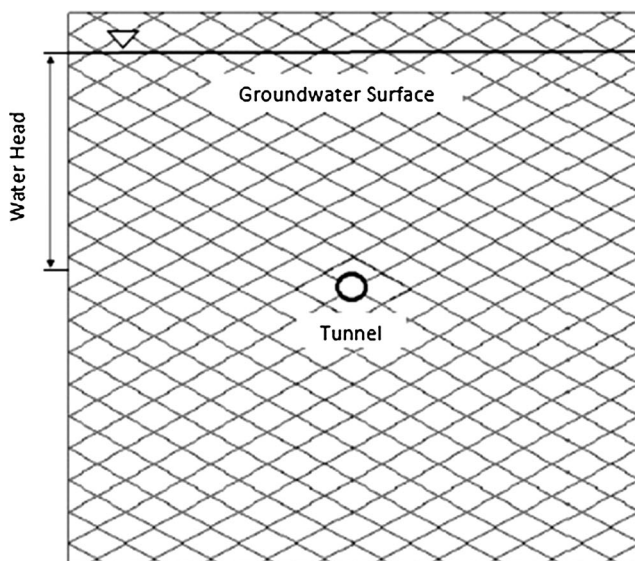


Fig. 4 Schematic section of the model domain, with the simulated joint sets

Table 2 Model parameters used in this study

Type of parameter	Parameter	Range of variation	
Geo-mechanical characteristic (with reference to the Mohr–Coulomb constitutive model chosen in the modeling)	Intact rock	Specific weight 26 kN/m ³ Bulk modulus 1.9 Gpa Shear modulus 1.74 Gpa	
	Joints	Normal and tangential stiffness 100 MPa/mm Friction angle 35 Cohesion Null	
	Geometrical characteristics of the discontinuity	Set number	2
		Set strike	Parallel to the tunnel axis (N–S)
		Set dip direction	Toward E or W
		Set dip	0°–90°
		Aperture	1×10^{-4} – 1×10^{-3} m ³
		Spacing	2–10 m
	Tunnel design parameters	Persistence	20–100 %
		Radius	1–10 m
Lining or waterproofing		Not present	
Depth		150 m	
Hydrogeological characteristics		Water table above tunnel	10–300 m
	Recharge	Not present	
	Joint Permeability	83.3 Pa ⁻¹ s ⁻¹	
	Mass density	1000 kg/m ³	
	Bulk modulus	2 GPa	

mechanically coupled). The solution for approximating the fluid flow rate through a joint relies on the classic Cubic Law, modified for the non-parallel wedge-shaped fractures. From the numerical simulations applying the above-mentioned boundary conditions, a conceptual model for a fully coupled hydro-mechanical discontinuity system can be derived.

Assessment of hydrogeological parameters impact on groundwater inflow

Due to the uncertainties in the measurement and analysis of rock mass characteristics, research on the impact of the uncertainty seems inevitable in the rate of flow through the rock masses. In line with this requirement, a more accurate

concept of problem was obtained by the sensitivity analysis on parameters affecting the water inflow on tunnel in order to determine the simulation permeability tensor and estimating the tunnel inflow in fractured rocks. Hence, in order to evaluate the uncertainty in measurements, any effective parameter increases by 10 and 20 % in each stage, while other parameters are constant and the impact of the increase on the rate of water flow into tunnel was investigated (Fig. 5). As shown in Fig. 5, increasing joint aperture and overburden have the maximum and minimum impacts on the water flow in the tunnel, respectively. Moreover, the effect of joint spacing is inverse. In other words, as the joint spacing increases, the rate of water inflow into the tunnel from the rock mass is decreased. In continue, sensitivity analyses of geo-structural parameters on the water inflow and the modeling results are discussed below.

Sensitivity analyses

By considering all the previously listed parameters and their related range of variation (Tables 1, 2), more than 750 simulations were carried out in relation to the joint set spacing, the tunnel radius, the hydraulic head, the dip direction/dip, joint aperture, joint trace and gap (Figs. 6, 7, 8). Results show that by increased degree of fracture (high frequency and low spacing), the tunnel inflow obviously increases. The simulations correctly reproduce the tunnel drainage in a rock mass. Also, for the same joint aperture, the growth rate of the discharge substantially depends on the orientation of discontinuities. It is noteworthy that the orientation of discontinuities significantly influences the direction of water flow: (1) when the hydraulic gradient is perpendicular to plane of the discontinuity, the discontinuity plane acts as an impermeable barrier and there is no water flow and, (2) the water flow is maximum along the gradient direction, if the plane of the discontinuity is parallel to the hydraulic gradient. The simulations revealed increase in the tunnel-water inflow with the increase of hydraulic head.

Many simulations were done by a constant joint aperture, coinciding with the soil surface. In this way, however, it was possible to simultaneously assess the influence of the joint aperture. The sensitivity analysis results showed significant effect of variations of this factor on the water inflow and that increased joint aperture results in sudden increase in the flow rate. As the tunnel radius decreases, the water flow rate decreases due to the reduced connected joint number. The study on geo-structural conditions showed that variations of the joint dip have significant impact on the water flow into the tunnel. In particular, the joint spacing is less, while the hydraulic head above the tunnel is high.

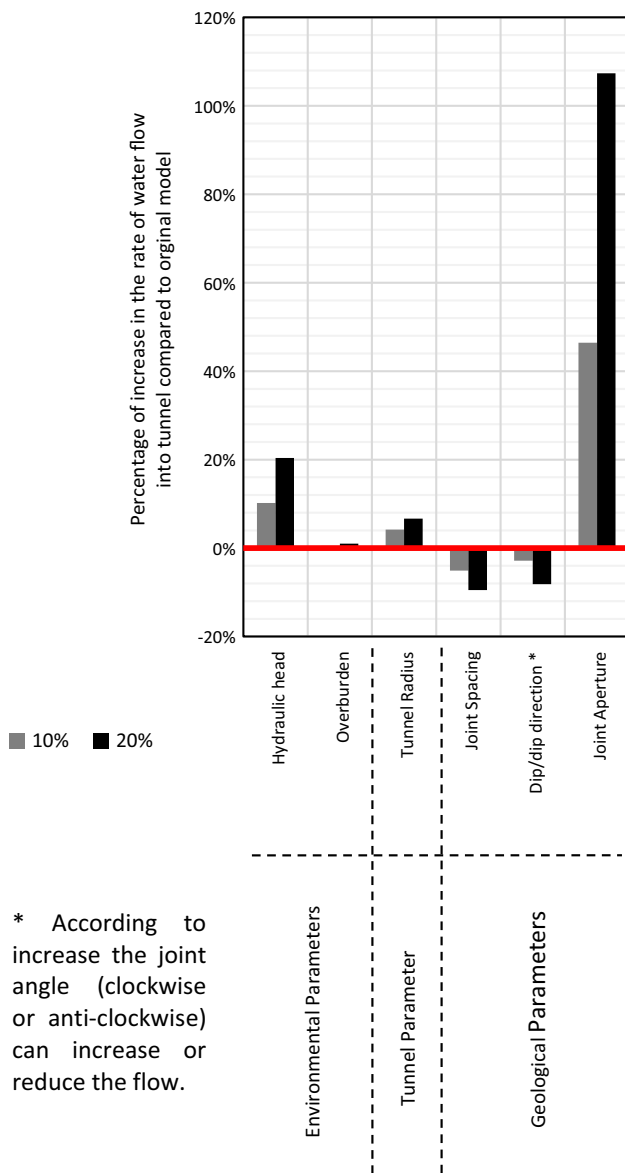


Fig. 5 Effect of increasing parameters on the groundwater inflow to the tunnel

Connectivity of joint networks

Joint connectivity is the key characteristic affecting the fluid flow in the jointed rock and refers to the degree of interconnection of a joint population (Long and Witherspoon 1985). Independent fractures behave as isolated bonds which do not have any contribution to the shift of the fluid mass. Interconnected discontinuities, on the contrary, have influence on the conductivity and the water flow through a fracture network formed by connected series of bonds (Scesi and Gattinoni 2009). The geometric connectivity depends on the length, orientation and density of the fractures. The simulation results showed that the tunnel

inflow decreases as the gap length increases and the joint trace length decreases (Fig. 7). Crossing and abutting fractures will increase the connectivity, blind or dead-end fractures. Connectivity can be quantified in terms of percolation theory. Network percolation is the conductance of random networks of conductors. Each of the conductors in the network can be opened or closed depending on a probability (Bruines 2003).

Therefore, an interconnectivity probability P from the percolation theory was also considered. It was calculated as the ratio between the node’s number in the partially-connected domain and the corresponding node’s number for a fully interconnected domain with similar geo-structural characteristics (Berkowitz and Balberg 1993). Obviously, the tunnel inflow increases with the interconnectivity probability through an approximately exponential trend (Fig. 8). For an interconnectivity probability between 0.5 and 0.6, abrupt changes are observed in tunnel inflows (even for several orders of magnitude), corresponding to the critical probability P_c . Below this P_c , the system was not connected and the flow was considered to be local (no longer contributes to the tunnel inflow). However, above the P_c , there is a percolating cluster that spans the whole system and the flow is interconnected.

Analyses and discussions

Definition of empirical model

According to the sensitivity analysis presented in previous section, it is found that hydraulic conductivity has a major impact on groundwater inflow to tunnels. Hence, for obtaining an empirical model in discontinuous media or in other word for modifying of analytical methods, hydraulic conductivity parameter should be modified according to geo-structural properties using numerical simulations. Therefore, for the same configurations used in the numerical model, the tunnel water inflow was calculated using the Goodman formula.

Goodman et al. (1965), considering a source and a sink for simulation of a draining tunnel in a homogeneous semi-infinite aquifer, obtained an analytical equation. They applied the equations of Polubarinova (1962) that are identical to the equations developed by Muskat (1937). Experimental tests were performed on tunnel driving in water tanks. One of the interesting points mentioned by Goodman et al. (1965) is the slight increase of water inflow with an increase in tunnel diameter. This equation is developed based on the following assumptions; the radius flow, no bedding in the rock, and accurate prediction of equivalent permeability (Kong 2011):

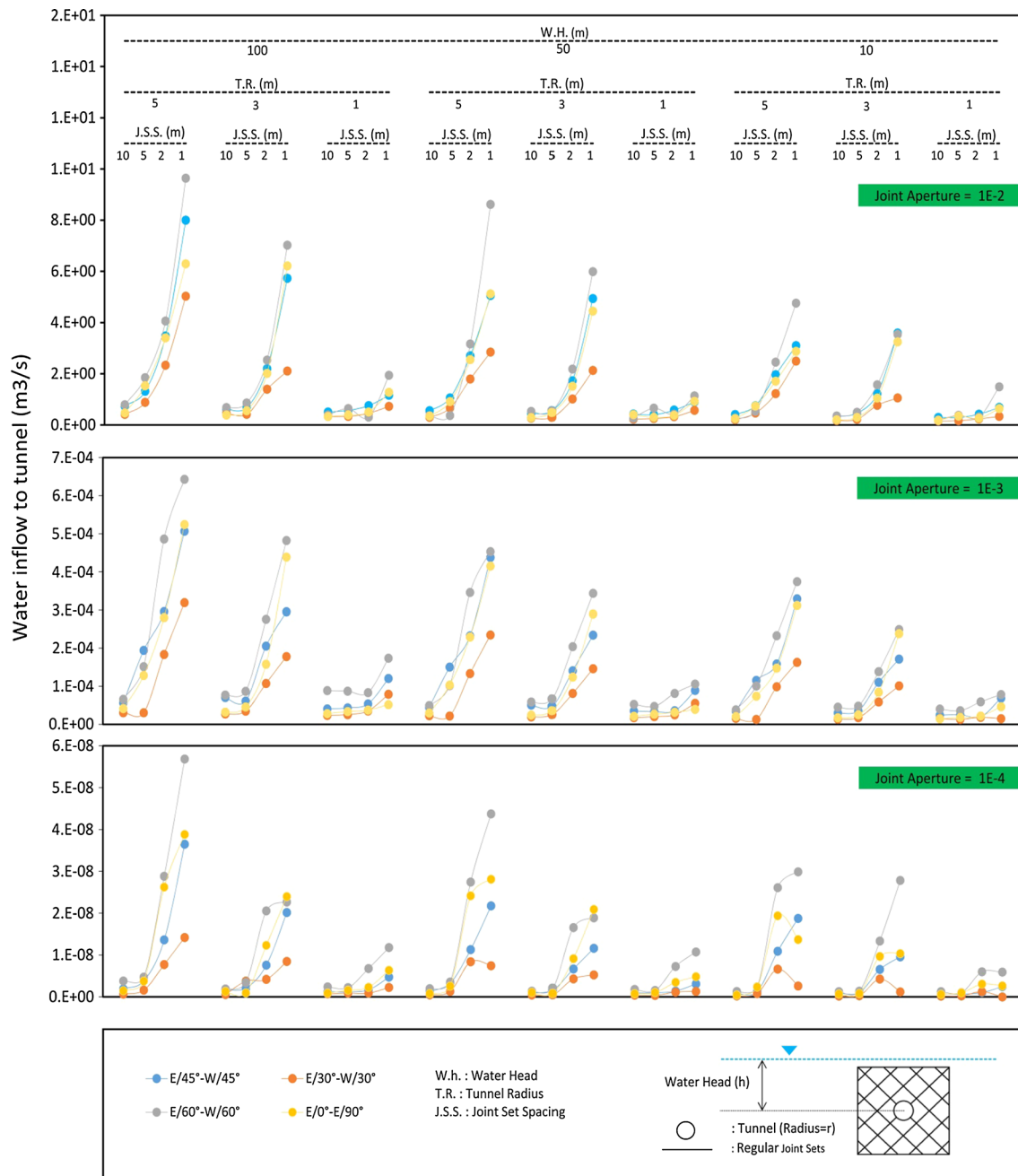


Fig. 6 Effect of significant parameters on groundwater flow into tunnel (hydraulic head W. H.: 10, 50, 100 m; tunnel radius T. R.: 1, 3, 5 m; joint set spacing J. S. S.: 1, 2, 5, 10 m; dip direction/dip: E/30°–

W/30°, E/45°–W/45°, E/60°–W/60°, E/0°–W/90°; joint aperture: 1×10^{-4} , 1×10^{-3} , 1×10^{-2} m)

$$Q = 2\pi K \frac{H}{2.3 \log\left(\frac{2h}{r}\right)} \tag{10}$$

In order to apply this equation, the equivalent hydraulic conductivity of the rock mass at the tunnel depth was calculated by Eq. (9). Comparison between the model results and those obtained through the Goodman analytical formula showed that the Goodman results significantly

overestimate the tunnel-water inflow, and that the greater this overestimation, the lower the joint dip will be (Fig. 9). As shown in Fig. 9, the simulated water inflow can be fitted as a function of the tunnel-water inflow, calculated by the analytical relations. To achieve this, a conditional function has to be defined in which the simulation of hydraulic conductivity depends on the geo-structural characteristics. Based on this comparison, an empirical relation was

Fig. 7 Trend of the tunnel inflow versus the joint gap for different values of joint trace length (L in legend) expressed in m and the joint trace length for different values of the gap (G in legend). All the results correspond to a geo-structural setting characterized by two conjugate joint sets ($E/30^\circ-W/30^\circ$) and spacing equal to 5 m

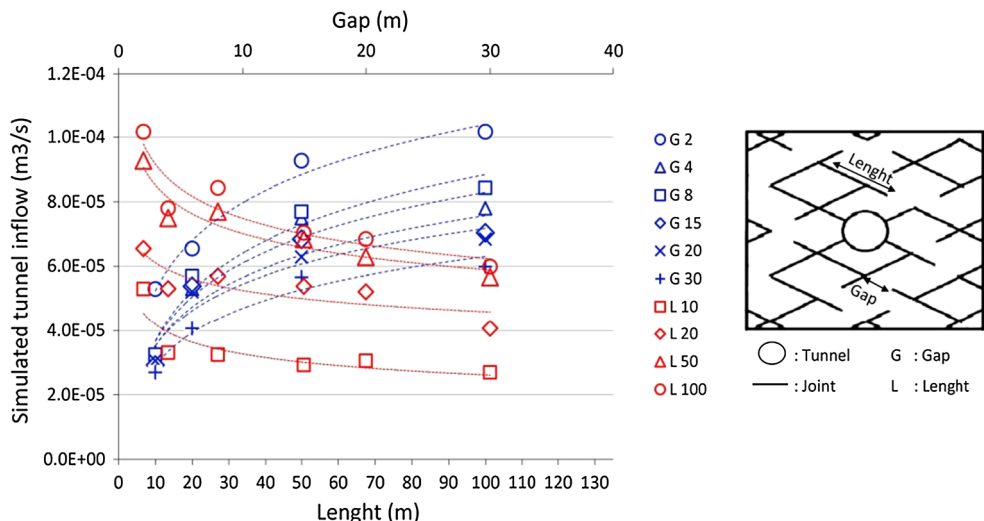


Fig. 8 Trend of the tunnel inflow versus the interconnectivity probability for different geo-structural settings, considering the joint spacing equal to 5 m. The gray band represents the critical probability P_c and in its left side, $P < P_c$, the flow will be localised, while in the right side, $P > P_c$, water inflow will be interconnected

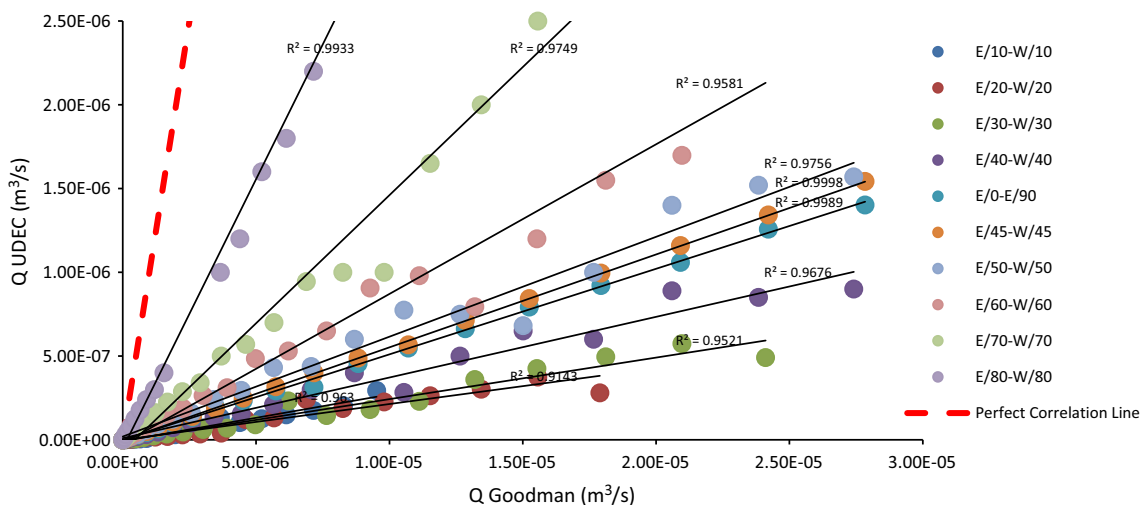
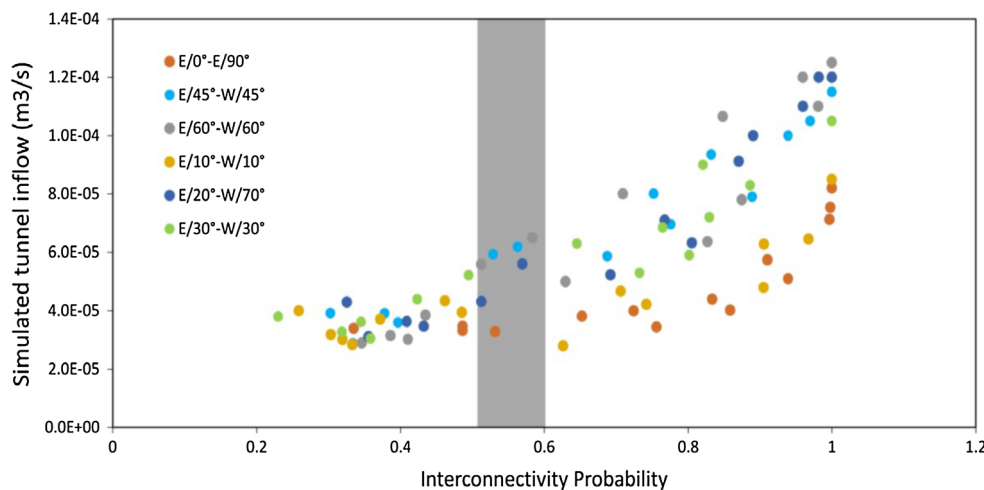


Fig. 9 The results of numerical analysis ($UDEC$) versus analytical prediction of groundwater inflow in different geostructural settings are demonstrated by coloured points. Continuous lines are drawn

based on linear regression. The regression coefficients as well as the red dotted line indicate the perfect correlation

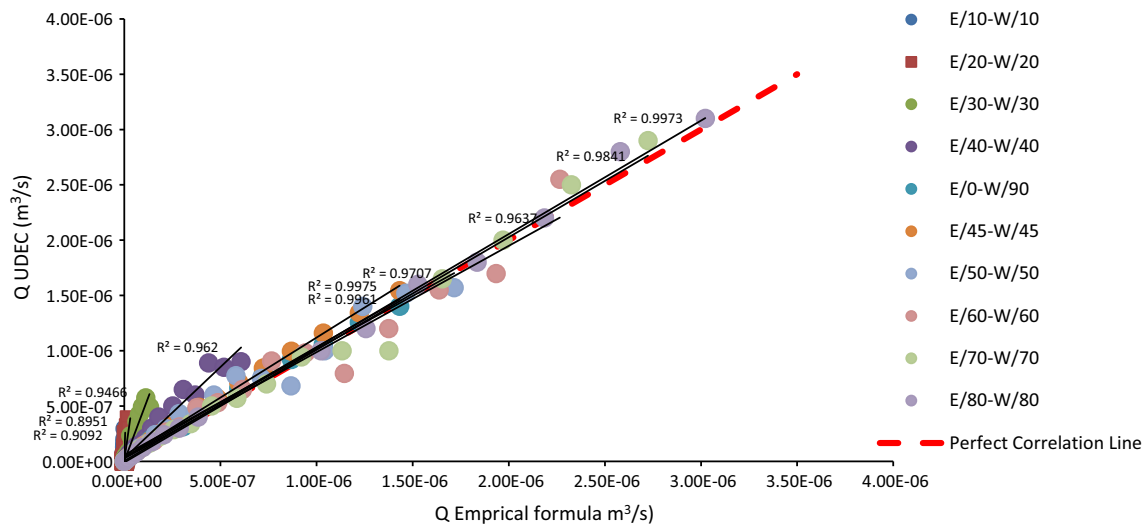


Fig. 10 Trend of the tunnel inflow using *UDEC* programme versus the inflow calculated through the empirical formula for several geo-structural conditions (characterized by two joint families and

changing dip). The *continuous lines* arise from the linear regression of the simulated values. The corresponding regression coefficients (R^2) and the *red dotted line* indicate a perfect correlation

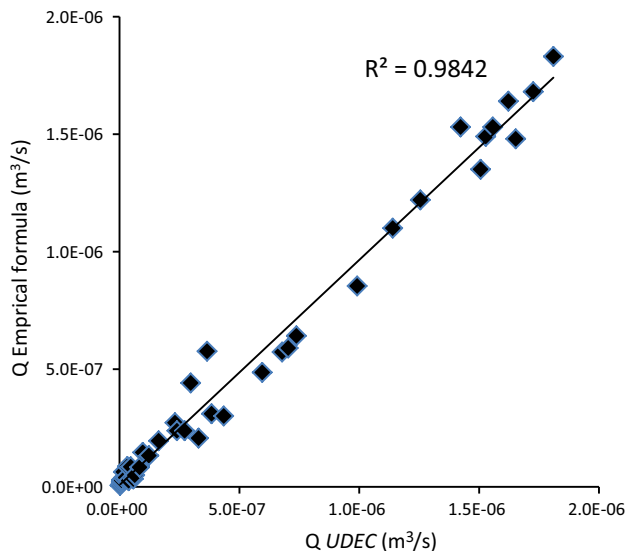


Fig. 11 The points represent the Q empirical formula versus the inflow calculated with the Q *UDEC* for the test data

proposed to estimate the tunnel water inflow, with particular reference to the case of depth below 150 m. For this depth and laminar regime, an increased dependence of the drainage process on the structural setting can be seen. Based on the Goodman equation, the following relation was defined:

$$Q_{em} = 2\pi k_{sim} \frac{H}{2.3 \log\left(\frac{2h}{r}\right)} \quad (11)$$

where Q_{em} (m^3/s) is the empirical tunnel inflow, and k_{sim} is the empirical hydraulic conductivity, used instead of k_{cq} in the analytical formula and depends on:

1. The joint dip,
2. The orientation of the hydraulic conductivity tensor.

To determine the K_{sim} , the following parameter λ was empirically defined:

$$\lambda = \begin{cases} K_{min} \sqrt{\frac{K_{min}}{K_{max}}} \cdot \left(1 - \cos(\theta_{min}) + \cos\left(\frac{\pi}{4}\right)\right)^{\sin(\theta_{min})}, & \theta_{min} \leq \frac{\pi}{4} \\ K_{min} \sqrt{\frac{K_{max}}{K_{min}}} \cdot \tan(\theta_{min}), & \theta_{min} > \frac{\pi}{4} \end{cases} \quad (12)$$

where K_{sim} and K_{max} are the minimum and maximum components of the hydraulic conductivity tensor, θ_{min} is the minimum joint dip and \varnothing_{min} is the angle between the K_{min} direction and the horizontal plane. λ is a conditional function based on the dip orientation. According to the regression analyses, the empirical K_{sim} defined as a function of λ :

$$K_{sim} = 0.055 - 1.64 \frac{\lambda}{Ln(\lambda)} - 0.055e^{\lambda} \quad (13)$$

$$R = 0.9765, R^2 = 0.9535$$

The statistics R and R^2 in the model Eq. (13) were in an acceptable range. Hence, the empirical equation (Eq. 11) was obtained considering geo-structural setting conditions (Fig. 10).

The fully interconnected-joints networks' empirical formula was extended to partially interconnected networks based on previously defined interconnectivity probability P :

$$Q_{em} = P^n 2\pi k_{sim} \frac{H}{2.3 \log\left(\frac{2h}{r}\right)} \quad (14)$$

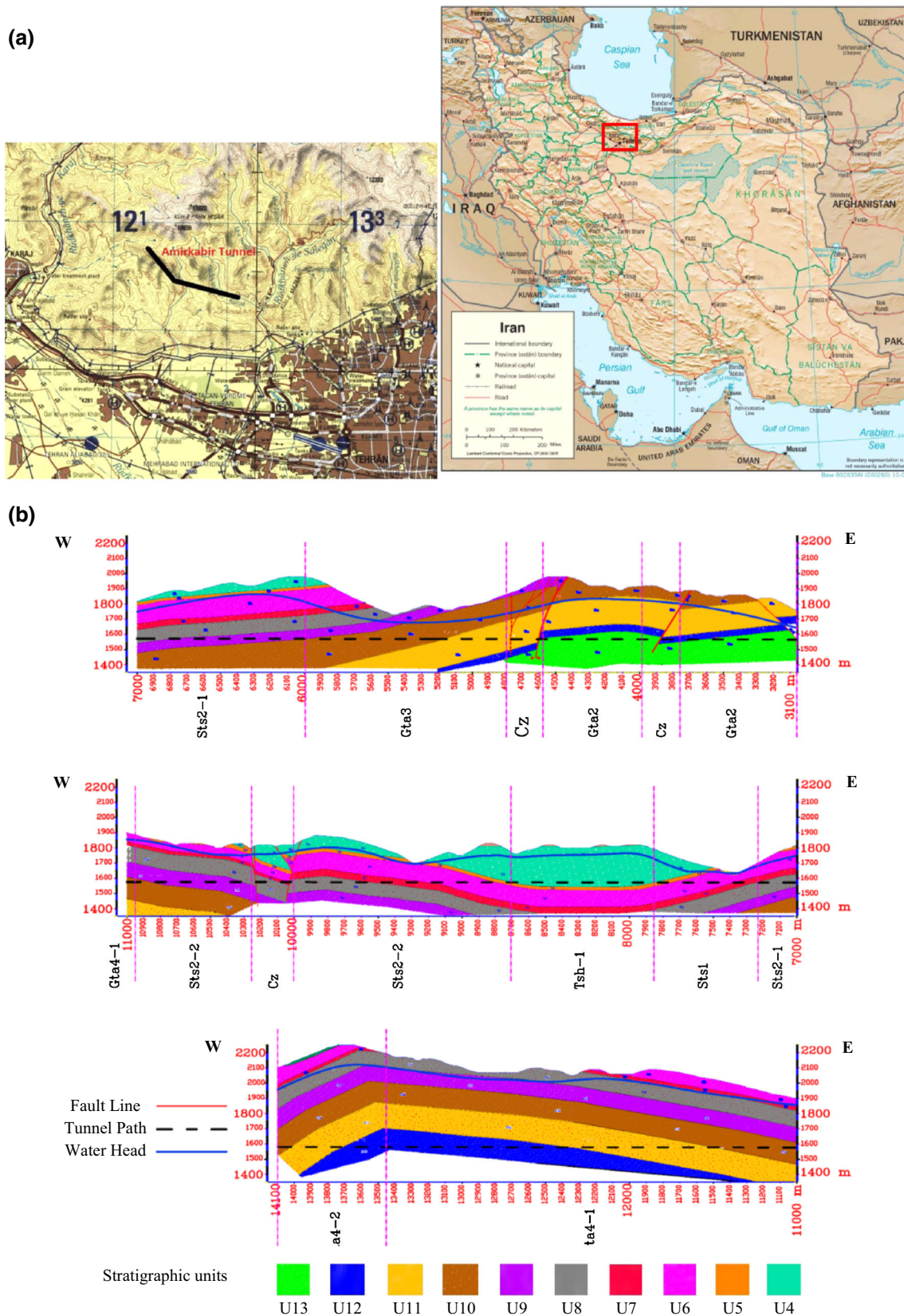


Fig. 12 Location (a) and geological section (b) of Amirkabir tunnel path (km 3.1–14.1) (SCE Company 2006)

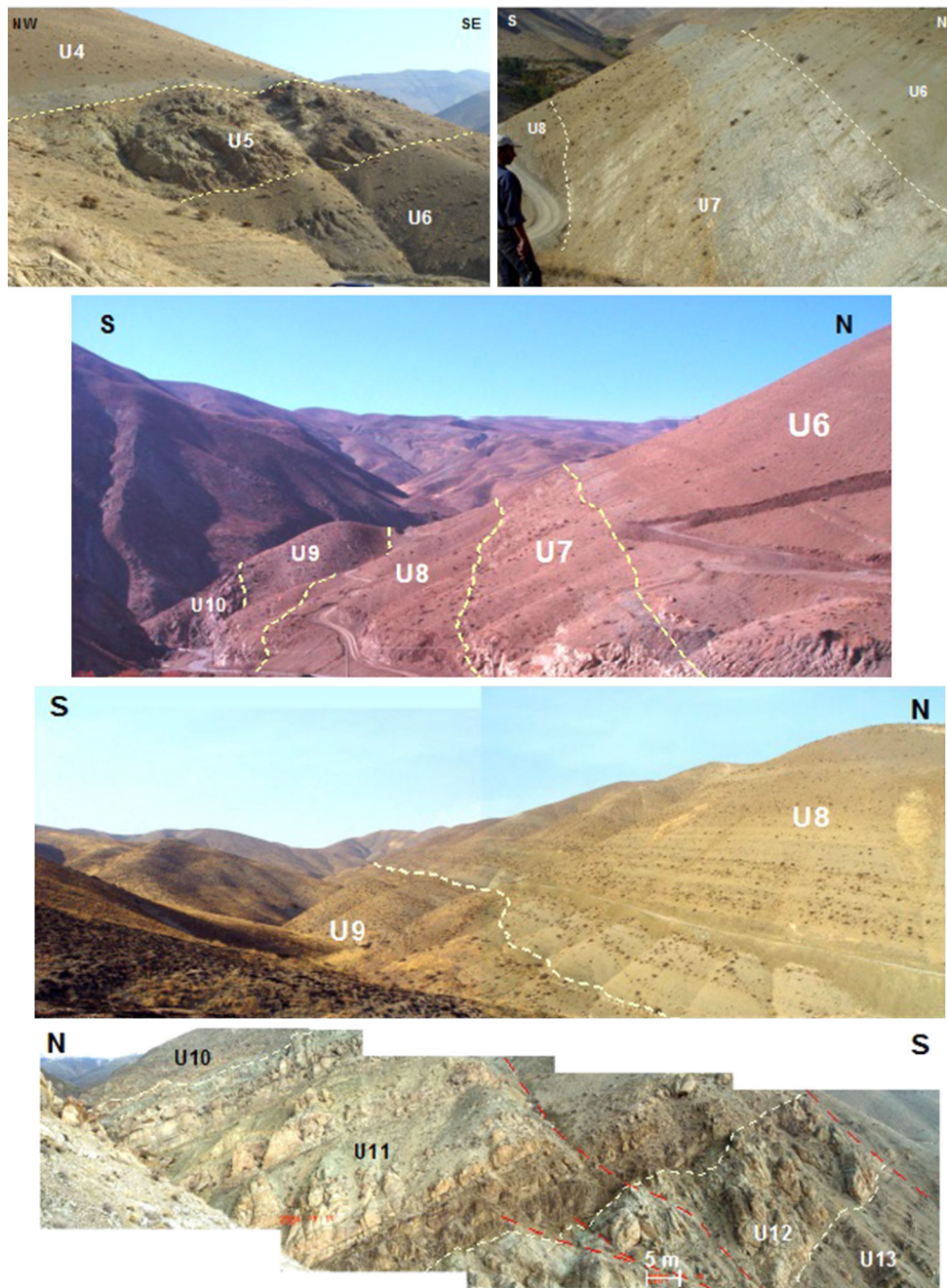


Fig. 13 Unit sequences from U₆ to U₁₀ in the study area showing different morphology of the tunnel site (SCE Company 2006)

where P is the probability of interconnectivity, previously defined and n is an empirical coefficient set out from the numerical results. The numerical results for the partially interconnected network and the tunnel inflow were compared with the empirical formula for different values of the exponent and it was revealed that the best estimation was achieved for $n = 2.5$. Equation (14) is valid only for $P \geq 0.5$. In fact, when P is lower than this percolation threshold ($P < P_c$), the flow is localized and it does not contribute to the tunnel inflow.

Model validation

After the model was acquired through the regression analyses, its accuracy Eq. (11) was evaluated on 30 % of the initial data, because the test data were excluded. Figure 11 shows the results of the Q empirical formula versus the Q numerical for the test data. As can be seen, the R^2 has an acceptable value; thus, the equation can be considered valid.

Table 3 Description of the tunnel site’s geological units (SCE company 2006)

No.	Stratigraphic units	Lithology	Engineering geological units	Description
1	U4	Alternation of this bedded shale, siltstone and sandstone	Gta1	Weak to moderately strong, thin to moderately bedded, intensely fractured, may be unstable
2	U5	Sandstone and micro-conglomerate	Gta2	Weak to moderately strong, thin to moderately bedded, moderately fractured, may be unstable
3	U6	Tuff siltstone	Gta3	Moderately strong to strong, moderately to thick bedded, slightly fractured, stable
4	U7	Massive green tuff		
5	U8	Siliceous green tuff and sandstone	Sts1	Weak to moderately strong, thin to moderately bedded, fractured, may be unstable
6	U9	Green vitric and lithic tuff and siltstone	Sts2	Very strong, thick bedded, stable
7	U10	Siliceous green tuff and sandstone		
8	U11	Sandstone and micro-conglomerate		
9	U12	Light cream lithic and vitric tuff	Tsh	Weak to moderately strong, thin to moderately bedded, foliated, fractured, may be unstable
10	U13	Sandstone, green vitric tuff and siliceous tuff	Cz	Weak to moderately strong, intensely fractured, unstable

Application to a real case

Numerical modeling of groundwater inflow to a tunnel could provide the best and precise results; however, it requires a detailed conceptual model of the hydrogeological condition, high costs and time-consuming simulations. As there are very limited amount of data in the preliminary geotechnical investigation of the site, it is better to define a simple equation that is able to consider the fractures network. This empirical equation, which is obtained based on parametrical modeling, makes the prediction of groundwater inflow as a function of joint characteristics available. The initial evaluation of the tunnel inflow is useful in determination of the highly risk areas from groundwater inflow point of view, where detailed investigations are necessary.

The results of the empirical equation were later applied to a real case (Amirkabir Tunnel, northern Iran). In geological studies, the tunnel intercept 14 geological units, which generally encompass various sedimentary-volcanic sets of Karaj formation. Its petrology contains layers of tuff, sandstone, fine-grained conglomerate, siltstones, lava and agglomerate. In this study, we investigated the groundwater inflow to tunnel from kilometers 3.1 to 14.1. Tunnel is divided to 9 engineering geological sections: Gta2 (sandstone and tuff layers), Gta3 (sandstone layers, tuff, and micro conglomerate), Gta4-1 (sandstone, tuff), Gta4-2 (tuff, in sandstone sections and micro conglomerate), Sts1 (tuff, siltstone, layers of sandstone and micro conglomerate), Sts2-1 (tuff, limestone), Sts2-2 (tuff, limestone, shale and siltstone), Tsh-1 (Sandstone, Shale, Silt stone) and Cz (tuff, sandstone, and micro conglomerate)

(Figs. 12, 13). Detailed description of geological units along the tunnel is presented in Table 3 and its geological profile is shown in Fig. 12 (SCE Company 2006).

For each tunnel section, Table 4 presents the hydraulic conductivity tensor. The corresponding surface equivalent hydraulic conductivity was calculated based on the geo-structural survey. This information was integrated with the results of 11 pumping tests (carried out in transient state with a constant rate at different depths). To measure the tunnel inflow using a flowmeter, the outflow was measured daily with synchronous advancing of drilling. Then, the tunnel inflow was calculated in different levels as the difference between the channel flow rate in the upstream and downstream levels. Calculation of tunnel water inflow was a possible task in each section with both Goodman’s equation and the new previously described empirical relation. A comparison was then performed between obtained results and the tunnel-monitoring data, arising from the flow rate measured in the tunnel channel at different tunnel distances. Considering the comparison results (Fig. 14), it is concluded that the tunnel water inflow is highly over-estimated using Goodman equation, especially in sections with higher rock mass anisotropy. The maximum hydraulic conductivity was in the direction close to the vertical. This overestimation was effectively corrected through the proposed empirical relation that provides values comparable to those actually observed in the tunnel. For example, “Materials and methods” section is derived in the intensely fractured area with the high rate of anisotropy. The comparison of the water inflow values obtained through Goodman and empirical equations with the observed water inflow rate show that the calculated groundwater inflow

Table 4 Main characteristics of different sections in Amirkabir tunnel (northern Iran), useful for the estimation of water inflows (1–12 refers to the divisional sections); (SCE company 2005)

	1	2	3	4	5	6	7	8	9	10	11	12
Location (km)	3.1–3.2	3.3–3.4	3.9–4	4.1–4.2	4.5–4.6	5.1–5.2	6.6–6.7	7.5–7.6	8.2–8.3	9.1–9.2	12–12.1	13.8–13.9
Length (m)	100	100	100	100	100	100	100	100	100	100	100	100
Average water table depth (m)	100	155	180	278	230	115	265	80	195	135	445	505
Tunnel depth (m)	240	280	325	325	405	185	310	100	215	165	475	625
Average joint set dip												
α_1 (°)	5	5	5	5	5	62	82	75	64	78	70	70
α_2 (°)	70	70	70	70	70	80	80	55	40	45	75	75
K_{eq} (m/s)	4.0E–07	4.0E–07	6.4E–06	4.0E–07	4.0E–07	8.6E–08	1.2E–07	8.4E–08	1.0E–07	1.9E–07	1.4E–08	1.4E–08
K_{min}/K_{max}	4.1E–01	4.1E–01	4.1E–01	4.1E–01	4.1E–01	2.5E–02	3.0E–04	3.1E–02	4.5E–02	8.8E–02	2.0E–03	2.0E–03
K_{min} (m/s)	2.5E–07	2.5E–07	4.E–06	2.5E–07	2.5E–07	1.4E–08	2.1E–09	1.5E–08	2.1E–08	5.5E–08	6.4E–10	6.4E–10
ϕ_{min}	37.5	37.5	37.5	37.5	37.5	71	80	85	76	61.5	72.5	72.5

rate using the empirical equation is closer than the inflow value computed by Goodman equation to the observed water inflow rate with the relative differences of 38 and 493 %, respectively. In other words, accurate estimation of hydraulic conductivity tensor in fractured and heterogeneous zones has a main impact on accuracy and precision of groundwater inflow prediction. These results confirm the importance of considering the discontinuous nature of the media, with particular reference to its structural setting.

Conclusions

In the recent decades, accurate prediction of groundwater inflow to the tunnel is of great interest in the engineering practice, especially for assessment of environmental impact and designation of tunnel drainage system. In this regard, various analytical equations exist in the technical literature; however, they do not accurately reflect the real phenomena since they are developed based on simplifying assumptions such as homogeneous aquifer, which is in contrast to the fractured nature of the rock masses in the perimeter of the tunnel.

The study aimed to define corrective hydraulic conductivity applicable to Goodman formula for tunnel inflow assessment. The rock-mass geo-structural setting was taken into account. The numerical flow model enabled identifying and quantifying the influence of different parameters (orientation of joint sets, joint spacing and aperture, tunnel radius, and hydraulic head) on the tunnel water inflow. The results show that the joint spacing and aperture mainly control the tunnel discharge. This dependency can still be efficiently reproduced by a single parameter, that is the equivalent hydraulic conductivity. The most interesting result is that the tunnel inflow depends on the geo-structural setting of the rock mass, especially when the joint spacing is less and the hydraulic head above tunnel is high. In particular, the faster the rate of tunnel flow increases with the equivalent hydraulic conductivity of the rock mass, the lesser is the joint set dip. Obviously, the geo-structural setting is one of the factors with highest influence on the drainage process, but it is rarely included in analytical approach. Hence, the only parameter covering aperture, orientation and spacing of the fractures is hydraulic conductivity which has a special role in prediction of groundwater inflow to tunnel. Thus, for obtaining an empirical model in discontinuous media or in other word for modifying of analytical methods, hydraulic conductivity parameter should be modified according to geo-structural properties using numerical simulations.

Numerical model results and analytical formulas were compared and a method was obtained to adapt the simple analytical equations of Goodman to the geo-structural

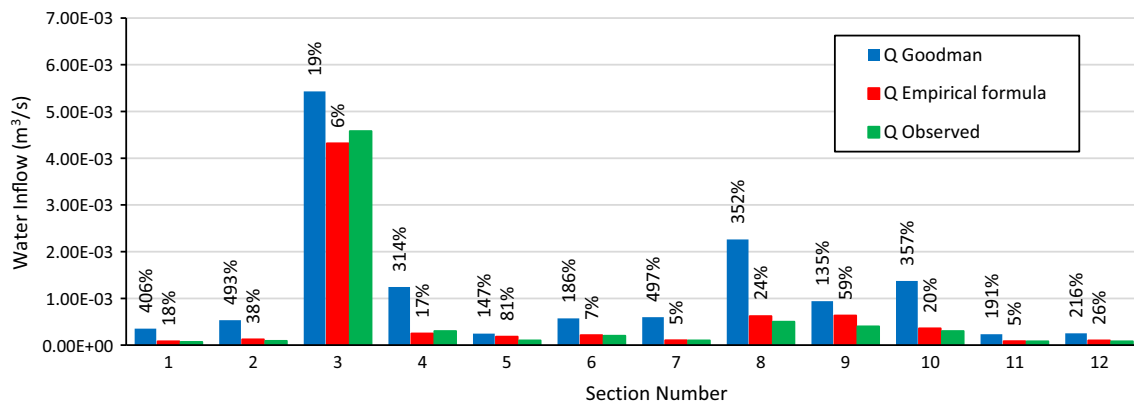


Fig. 14 Comparison between observed water inflow at amirkabir tunnel (in green), calculated using Goodman equation (in blue) and the empirical relation (in red). The percentage values on the

chart demonstrate the relative difference of the inflow rates calculated using the Goodman and empirical formulas with the observed water inflow rates in each section

characteristics of the rock mass. To achieve the project aim, numerical simulation was done and a sufficient data set was developed to calibrate Goodman equation and/or define empirical relation according to various structural and geological conditions. This equation was calibrated with respect to average depth of the tunnel, equal to 150 m and normal effective stress of 2–3 MPa. This equation was acquired for fully interconnected fractures network and then, was extended to partially interconnected network, considering the interconnectivity probability. Finally, the empirical and analytical relations were used to estimate the water inflow into Amirkabir tunnel as a case study and was compared to the monitoring data. Some sections of this case study were derived on intensely fractured rock mass. The outcomes of empirical relation corresponded to the monitoring data, especially in those tunnel sections with high anisotropy of rock mass. Therefore, of particular note is that according to geostructural properties of discontinuous media using modified hydraulic conductivity in Goodman solution, a more precise prediction of groundwater inflow to tunnel and as a consequence, a lower relative difference in comparison to the observed inflow rate is reasonable.

References

Alejano R (2014) Rock engineering and rock mechanics: structures in and on rock masses. CRC Press. ISBN: 113800149X, 978-1-138-00149-7, 978-1-315-74952-5

Andersson J, Dverstorp B (1987) Conditional simulations of fluid flow in three-dimensional network of discrete fractures. Water Resour Res 23:1876–1886. doi:10.1029/WR023i010p01876

Bear J (1993) Modelling flow and contaminant transport in fractured rocks. In: Bear J, Tsang CF, DeMarsily G (eds) Flow and contaminant transport in fractured rock. Academic Press, San Diego

Berkowitz B, Balberg I (1993) Percolation theory and its application to ground hydrology. Water Resour Res 29(4):775–794. doi:10.1029/92WR02707

Blessent D, Therrien R, MacQuarrie K (2009) Coupling geological and numerical models to simulate groundwater flow and contaminant transport in fractured media. Comput Geosci 35(9):1897–1906. doi:10.1016/j.cageo.2008.12.008

Bruines P (2003) Laminar ground water flow through stochastic channel networks in rock. PhD thesis, EPFL

Butscher CH (2012) Steady-state groundwater inflow into a circular tunnel. Tunn Undergr Space Technol 32:158–167. doi:10.1016/j.tust.2012.06.007

Cacas MC, Ledoux E, DeMarsily G, Tillie B, Barbreau A, Durand E, Feuga B, Peaudecerf P (1990) Modeling fracture flow with a stochastic discrete fracture network: calibration and validation 1. The flow model. Water Resour Res 26(3):479–789. doi:10.1029/WR026i003p00479

Cesano D, Bagtzoglou AC, Olofsson B (2003) Quantifying fractured rock hydraulic heterogeneity and groundwater inflow prediction in underground excavations: the heterogeneity index. Tunn Undergr Space Technol 18:19–34

Coli M, Pinzani A (2012) Tunnelling and hydrogeological issues: a short review of the current state of the art. Rock Mech Rock Eng. doi:10.1007/s00603-012-0319-x

Croci A, Francani V, Gattinoni P (2003) Studio idrogeologico del bacino del Torrente Esino. Quaderni di Geologia Applicata 10(2):148–166

Dunning CP, Feinstein DT, Hunt RJ, Krohelski JT (2004) Simulation of ground-water flow, surface-eater flow, and a deep sewer tunnel system in the Menomonee Valley, Milwaukee, Wisconsin. US Geol Surv Sci Invest Rep 2004-5031

Dverstorp B, Andersson J (1989) Application of the discrete fracture network concept with field data: possibilities of model calibration and validation. Water Resour Res 25(3):540–550. doi:10.1029/WR025i003p00540

El Tani M (2003) Circular tunnel in a semi-infinite aquifer. Tunn Undergr Space Technol 18:49–55. doi:10.1016/S0886-7798(02)00102-5

El Tani M (2010) Helmholtz evolution of a semi-infinite aquifer drained by a circular tunnel. Tunn Undergr Space Technol 25:54–62. doi:10.1016/j.tust.2009.08.005

Fernandez G, Moon J (2010) Excavation-induced hydraulic conductivity reduction around a tunnel, part 1: guideline for estimate of ground water inflow rate. Tunn Undergr Space Technol 25(5):560–566. doi:10.1016/j.tust.2010.03.006

- Garzonio CA, Piccinini L, Gargini A (2014) Groundwater modeling of fractured aquifers in mines: the case study of gavorrano (Tuscany, Italy). *Rock Mech Rock Eng* 47:905–921. doi:10.1007/s00603-013-0444-1
- Gattinoni P, Scesi L (2010) An empirical equation for tunnel inflow assessment: application to sedimentary rock masses. *Hydrogeol J* 18:1797–1810. doi:10.1007/s10040-010-0674-1
- Gattinoni P, Scesi L, Terrana S (2008) Hydrogeological risk analysis for tunneling in anisotropic rock masses. In: Proceedings of the ITA-AITES world tunnel congress, underground facilities for better environment & safety, Arga, India, 1736–174
- Goodman R, Moye D, Schalkwyk A, Javendel I (1965) Groundwater inflow during tunnel driving. *Eng Geol* 1:150–162
- Herbert AW (1996) Modelling approaches for discrete joint network flow analysis. Coupled thermo-hydro-mechanical process of jointed media. Elsevier, Philadelphia. ISBN 978-0-444-82545-2
- Holmoy KH, Nilsen B (2014) Significance of geological parameters for predicting water inflow in hard rock tunnels. *Rock Mech Rock Eng* 47:853–868. doi:10.1007/s00603-013-0384-9
- Hung C, Evans DD (1985) A 3-dimensional computer model to simulate fluid flow and contaminant transport through a rock fracture system. NUREG/CR-4042, US Nuclear Regulatory Commission
- Hwang JH, Lu CC (2007) A semi-analytical method for analyzing the tunnel water inflow. *Tunn Undergr Space Technol* 22(1):39–46. doi:10.1016/j.tust.2006.03.003
- Itasca (2011) Universal distinct element code (UDEC) user's guide, 3rd edn. Itasca Consulting Group Inc., Minneapolis
- Jacob CE, Lohman SW (1952) Nonsteady flow to a well of constant drawdown in an extensive aquifer. *Trans Am Geophys Union* 33(4):559–569. doi:10.1029/TR033i004p00559
- Kong WK (2011) Water ingress assessment for rock tunnels: a tool for risk planning. *Rock Mech Rock Eng* 44(6):755–765. doi:10.1007/s00603-011-0163-4
- Kraemer SR, Haitjema HM (1989) Regional modelling of fractured rock aquifers. In: Jousma G et al (eds) *Groundwater contamination: use of models in decision-making*. Kluwer Academic Publishers, Dordrecht
- Liao QH, Hencher SR (1997) Numerical modelling of the hydro-mechanical behaviour of fractured rock masses. *Int J Rock Mech Min Sci* 34(3–4):177.e1–177.e17. doi:10.1016/S1365-1609(97)00052-X
- Liu F, Xu G, Huang W, Hu Sh, Hu M (2012) The effect of grouting reinforcement on groundwater seepage in deep tunnels. *Blucher Mech Eng Proc* 1(1):4727–4737
- Long JCS, Witherspoon PA (1985) The relationship of the degree of interconnection to permeability in fracture networks. *J Geophys Res* 90:3087–3098. doi:10.1029/JB090iB04p03087
- Louis C (1974) Introduction à l'hydraulique des roches [Introduction to rock hydraulics]. *Bur Rech Geol Min* 4(III):283–356
- Marechal JC, Perrochet P (2003) New analytical solution for the study of hydraulic interaction between Alpine tunnels and groundwater. *Bull Soc Géol Fr* 174(5):441–448. doi:10.2113/174.5.441
- Molinero J, Samper J, Juanes R (2002) Numerical modeling of the transient hydrogeological response produced by tunnel construction in fractured bedrocks. *Eng Geol* 64:369–386
- Muskat M (1937) *The flow of homogeneous fluids through porous media*. McGraw Hill, New York, pp 175–181
- Palmstrom A, Stille H (2007) Ground behavior and rock engineering tools for underground excavations. *Tunn Undergr Space Technol* 22:363–376. doi:10.1016/j.tust.2006.03.006
- Papini M, Scesi L, Bianchi B (1994) Studi finalizzati alla previsione delle venute d'acqua in galleria. *Costruzioni*
- Park K, Owatsiriwong A, Lee JG (2008) Analytical solution for steady-state groundwater inflow into a drained circular tunnel in a semi-infinite aquifer: a revisit. *Tunn Undergr Space Technol* 23:206–209. doi:10.1016/j.tust.2007.02.004
- Perrochet P, Dematteis A (2007) Modeling transient discharge into a tunnel drilled in heterogeneous formation. *Ground Water* 45(6):786–790. doi:10.1111/j.1745-6584.2007.00355.x
- Polubarinova KPA (1962) *Theory of ground water movement*. Translated by De Wiest RJM. Princeton University, Princeton
- Rasmussen TC (1988) Fluid flow and solute transport through three-dimensional networks of variably saturated discrete fractures. Ph.D. Dissertation, University of Arizona
- Ribacchi R, Graziani A, Boldini D (2002) Previsione degli afflussi d'acqua in galleria ed influenza sull'ambiente. In: Barla & Barla (ed) *Le Opere in Sottterraneo e il Rapporto con l'Ambiente*, 143–199
- Robinson PC (1982) Connectivity of fracture system—a percolation theory approach. Theoretical Physics Division, AERE Arwell. DOE Report No. DOE/RW/81.028
- Samardzioska T, Popov V (2005) Numerical comparison of the equivalent continuum, non homogeneous and dual porosity models for flow and transport in fractured porous media. *Adv Water Resour* 28(3):235–255. doi:10.1016/j.advwatres.2004.11.002
- SCE Company (2005) Site hydrogeology reports for KRJ project
- SCE Company (2006) Geological and engineering geological reports for KWCT project Project (Lot1), unpublished report
- Scesi L, Gattinoni P (2009) *Water circulation in rocks*. Springer. ISBN: 9789048124169
- Snow DT (1969) Anisotropic permeability of fractured media. *Water Resour Res* 5(6):1273–1289. doi:10.1029/WR005i006p01273
- Therrien R, Sudicky EA (1996) Three-dimensional analysis of variably-saturated flow and solute transport in discretely fractured porous media. *J Contam Hydrol* 23(1–2):1–44
- Zangerl C, Eberhardt E, Evans KF, Loew S (2008) Consolidation settlements above deep tunnels in fractured crystalline rock: part 2, numerical analysis of the Gotthard highway tunnel case study. *Int J Rock Mech Min Sci* 45:1211–1225. doi:10.1016/j.ijrmm.2008.02.005
- Zhang L, Franklin JA (1993) Prediction of water flow into rock tunnels: an analytical solution assuming a hydraulic conductivity gradient. *Int J Rock Mech Min Sci* 30(1):37–46. doi:10.1016/0148-9062(93)90174-C
- Zhang X, Sanderson DJ, Harkness RM, Last NC (1996) Evaluation of the 2-D permeability tensor for jointed rock mass. *Int J Rock Mech Min Sci* 33(1):17–37. doi:10.1016/0148-9062(95)00042-9